Ferrocene-1, 1′-dithiol as molecular wire between Ag electrodes: The role of surface defects

T. Bredow, C. Tegenkamp, H. Pfnür, J. Meyer, V. V. Maslyuk, and I. Mertig

Citation: The Journal of Chemical Physics **128**, 064704 (2008);
View online: https://doi.org/10.1063/1.2827867
View Table of Contents: http://aip.scitation.org/toc/jcp/128/6
Published by the American Institute of Physics

Ferrocene-1,1′-dithiol as molecular wire between Ag electrodes: The role of surface defects

T. Bredow
Institut für Physikalische und Theoretische Chemie, Universität Bonn, Wegelerstr. 12, D-53115 Bonn, Germany

C. Tegenkamp[a] and H. Pfnür
Institut für Festkörperphysik, Leibniz Universität Hannover, Appelstraße 2, D-30167 Hannover, Germany

J. Meyer
Fritz Haber Institut der Max Planck Gesellschaft, Abteilung Theorie, Faradayweg 4-6, D-14195 Berlin, Germany

V. V. Maslyuk and I. Mertig
Fachbereich Physik, Martin-Luther-Universität Halle-Wittenberg, D-06099 Halle, Germany

(Received 25 October 2007; accepted 28 November 2007; published online 11 February 2008)

The interaction of ferrocene-1,1′-dithiol (FDT) with two parallel Ag(111) surfaces has been theoretically studied at density-functional level. The effect of surface defects on the energetic and electronic structure was investigated. The electronic transport properties are studied with the nonequilibrium Green's function approach. The adsorption geometry has a strong effect on the electronic levels and conductivity. The presence of point defects strongly enhances the molecule-surface interaction but has a surprisingly small effect on the density of states near the Fermi energy. The FDT-surface bond is particularly strong near terraces or steps and leads to significant shifts of the molecular orbitals relative to the gas phase. For all considered defect types except the single adatom the electronic conductivity through the FDT molecule is decreased compared to adsorption on perfect surfaces. © *2008 American Institute of Physics*.
[DOI: 10.1063/1.2827867]

I. INTRODUCTION

The binding of molecules to a metallic surface is one of the longstanding key issues relevant in fields such as catalysis,[1] corrosion,[2] friction,[3] or photochemistry.[4] By identification of relevant model systems that are accessible to quantitative simulations an insight into many detailed mechanisms has been made possible in recent years.

Details of the binding of molecules to metallic surfaces turn out to be also of high relevance to electron transport through single molecules,[5] that may eventually be functionalized as molecular conductors or even as switches inducing conformational changes by external electric fields or light.[6] This is due to the fact that in the absence of additional excitations, e.g., by light, only the small section of the molecular energy spectrum in the immediate neighborhood of the Fermi level of metallic electrodes is of relevance to electric transport through the molecule. In a many electron system consisting of molecule plus electrodes an intricate interplay between binding strength, local coordination, density of states (DOS) close to the Fermi level, overlap of wave functions, and conductance exists, and our understanding of this interplay is very incomplete. Although metal electrodes are usually crystalline at a microscopic level, the situation is complicated by the fact that defects at the electrode surfaces like point defects and steps must be taken into account. The study presented here in fact emphasizes their importance. Finally, as we will discuss at the end of this paper, the question arises whether conducting and nonconducting molecules of the same sort, but with different coordinations on the metal surface, can be present. In this case, also lateral interactions between the adsorbed molecules must be taken into account, which is beyond the scope of the present study.

In a recent study we investigated the adsorption of ferrocene-1,1′-dithiol (FDT) at the perfect Ag(111) surface.[7] This system was chosen since ferrocene based molecules exhibit a remarkably large conductance without activation thresholds[8,9] and a high structural flexibility with respect to rotation of the two cyclopentadienyl (Cp) rings. This was part of an investigation of FDT based molecules acting as molecular wires between silver electrodes.

In this study, we investigate the adsorption of FDT between two perfect and defective Ag(111) surfaces using the density-functional theory. As possible defects Ag vacancies, single adatoms (tip configuration), small islands, and monoatomic steps have been taken into account. Based on the experience from our previous study we consider the molecule-surface contact via the sulfur atoms. In most cases we considered S–H dissociation, i.e., a dithiolate was adsorbed. This situation was found to be only slightly more stable than molecular adsorption on perfect Ag(111) surfaces[7] but lead to much better overlap between the molecular orbitals and the silver levels near the Fermi energy.

[a]Electronic mail: tegenkamp@fkp.uni-hannover.de

TABLE I. Calculated dithiolate binding energies E_B, reaction energies $\Delta E^{\text{thiolat}}$ and ΔE^{thiol} (eV), optimized Ag-interlayer (contact) distance ΔZ, and nearest S–Ag distances R (Å).

Surface model	E_b	$\Delta E^{\text{thiolat}}$	ΔE^{thiol}	ΔZ	$R_{\text{S,Ag}}$
Ag 4×4×4 parallel	2.40	−0.29	−0.23	8.9	2.59,2.59/2.58, 2.58,2.56
Ag 4×4×4 perpendicular	2.47	−0.36	−0.36	10.3	2.58,2.61/2.56
Ag 4×4×4 Ag defect parallel	3.14	−1.03		8.7	2.60,2.72
Ag 4×4×4 Ag defect perpendicular	2.91	−0.80		9.9	2.55,2.62/2.79
Ag 4×4×5+(1×1) adatom (tip)	2.42	−0.31		10.8	2.43
Ag 4×4×5+(2×2) side on	3.24	−1.13	−0.40	10.3	2.47,2.52
Ag 4×4×5+(2×2) centered	2.79	−0.68		11.2	2.70,2.85
Ag 6×4×2+(4×4×1) step	3.01	−0.90		11.0	2.55,2.59

For one case (side-on adsorption of FDT on small silver islands) we also investigated molecular adsorption.

II. TECHNICAL DETAILS

Our calculations were performed within the density functional theory employing the generalized gradient approximation (GGA) for the exchange correlation functional as given by Perdew and Wang[10] and Perdew *et al.*[11] as implemented in the VASP code.[12–15] Plane waves in combination with the projector augmented wave method[16,17] have been used in order to expand the eigenstates.

Most of the computational parameters were the same as described in the previous study:[7] The number of plane waves was limited by a cut-off energy of 400 eV. All calculations were carried out without spin polarization. Surfaces were modeled within the supercell approach. The basic model is a 4×4 slab of the primitive Ag(111) surface unit cell with four atomic layers and 15 Å of vacuum. Brillouin zone integrations were performed using a (3×3×1) Monkhorst-Pack grid[18] or equivalent sets of special *k*-points when the cell size needed to be modified. Smearing according to the scheme of Methfessel and Paxton[19] with a smearing width decreased to 0.05 eV compared to the previous study[7] has been employed. The positions of all atoms have been relaxed until forces on each atom were smaller than 0.02 eV/Å. DOSs have been extracted from the relaxed structures using P4VASP.[20]

With the present computational setup the calculated Ag bulk lattice constant is 4.16 Å, slightly overestimating the experimental value of 4.09 Å (Ref. 21) as typical for gradient corrected functionals. The calculated surface energy is 0.344 eV/atom.

In order to model the adsorption of FDT between two Ag electrodes, we benefit from the periodicity along the surface normal. Rather than defining an electrode distance arbitrarily, we used the corresponding cell parameter as a variational parameter in our calculations. In this way, we could obtain an optimal bonding between the two sulfur atoms of FDT and the two sides of the silver slab.

The transport property calculations were done with the TRANSIESTA package.[22] It combines the nonequilibrium Green's function formalism[23] with the density functional theory which is implemented in the SIESTA code.[24] We use the Perdew-Burke-Ernzerhof[25] exchange-correlation functional and 400 Ry energy cutoff to define real-space grid for the density manipulation. A TZP basis set was used for the iron atom and DZP basis set was used for all other elements. 3*p* states were added as valence in the pseudopotential of Fe.

Regarding the transport calculations the system was divided into three regions, namely, left and right semi-infinite electrodes and a central scattering region containing the FDT molecule and the Ag surface atoms. As surface we define the first three Ag layer, whereas the next layers correspond to the bulk. Our test calculations have shown that a further increase of the number of layers in the surface does not change the results significantly. Taking into account that the left and right leads are in equilibrium and can be described with self-energies $\hat{\Sigma}_L$ and $\hat{\Sigma}_R$ we can define the Green's function of the scattering region in the presence of the leads as

$$\hat{G}(z) = (z\hat{S} - \hat{H}[\rho] - \hat{\Sigma}_L - \hat{\Sigma}_R)^{-1}, \tag{1}$$

where $\hat{S}$ and $\hat{H}$ are the overlap matrix and DFT Hamiltonian, respectively, and $z=e+i\delta$ with $\delta \to 0$. This allow us to evaluate the following density matrix:

$$\rho = \int dz \hat{G}(\hat{\Gamma}_L + \hat{\Gamma}_R)\hat{G}^{\dagger}, \tag{2}$$

where $\hat{\Gamma}_{L/R} = i(\hat{\Sigma}_{L/R} - \hat{\Sigma}^{\dagger}_{L/R})$ and to calculate the transmission spectra $T(E) = \hat{\Gamma}_L \hat{G} \hat{\Gamma}_R \hat{G}^{\dagger}$. Since the DFT Hamiltonian depends solely on the density matrix, Eqs. (1) and (2) can be iterated until reaching self-consistency.

III. RESULTS AND DISCUSSION

A. Structure and stability

In the following the results of structure optimizations for ferrocene dithiolate adsorption between two parallel Ag(111) surfaces with and without defects are described. Defects are isolated Ag vacancies, Ag adatoms, small Ag islands, and monoatomic steps. The calculated interaction energies are summarized in Table I. The reaction energies $\Delta E^{\text{thiolat}}$ and ΔE^{thiol} were obtained from the following reactions:

$$\Delta E^{\text{thiol}} = E(\text{Fe}(\text{C}_5\text{H}_4\text{SH})_2\text{:Ag}) - E(\text{Fe}(\text{C}_5\text{H}_4\text{SH})_2\text{(g)}) - E(\text{Ag}),$$

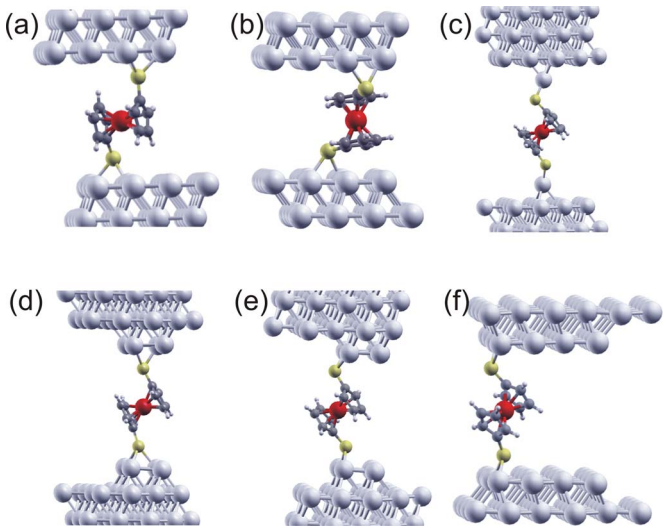

FIG. 1. (Color online) Optimized structures of FDT between two Ag(111) surfaces: (a) Cp axis parallel to defect-free (111) and (b) Cp axis perpendicular to (111). (c) Adsorption on single adatom, (d) centered on 2×2 terraces, (e) side-on the 2×2 structure, and (f) at steps. The Ag vacancy structure is not shown.

$$\Delta E^{\text{thiolat}} = E(\text{Fe}(\text{C}_5\text{H}_4\text{S})_2{:}\text{Ag}) + E(\text{H}_2(\text{g})) - E(\text{Fe}(\text{C}_5\text{H}_4\text{SH})_2(\text{g})) - E(\text{Ag}). \quad (3)$$

According to our definition, negative values of ΔE denote stabilization of the total system due to adsorption. In these calculations the same vectors were used for the cells of the surface-adsorbate system, the corresponding bare surface, and the isolated molecular species. The gas-phase molecules were fully optimized as described earlier.[7] The interaction energy E_b between ferrocene dithiolate and the surface is calculated with the biradical $\text{Fe}(\text{C}_5\text{H}_4\text{S})_2$ in its triplet ground state as reference. The hydrogen atoms removed from the S–H bonds were assumed to desorb as H_2 from the surface. For each surface model the lattice parameter c along the surface normal was numerically optimized.

Perfect Ag(111) surfaces could be adequately modeled using a $4\times4\times4$ slab. Two adsorption modes were considered, with the fivefold axis of the Cp rings[26] parallel and perpendicular to the Ag(111) surface [Figs. 1(a) and 1(b), respectively]. In the first mode only the S atoms of FDT are in close contact with the surface atoms, while in the second mode also an interaction via the Cp rings is possible. When comparing the relative energies of the two modes one has to bare in mind that DFT approaches tend to underestimate dispersion interactions between aromatic rings and metal surfaces (see, e.g., Ref. 27). Within the assumed error bars of the methods the reaction energies $\Delta E^{\text{thiolat}}$, −0.36 and −0.29 eV, are indistinguishable. However, changes in configurational interactions of the Cp rings are seen partly by broadenings in the DOS structure (see below).

To simulate single *Ag vacancies*, two silver atoms were removed from the first and the fourth layers of the $4\times4\times4$ slab. We chose identical lateral positions for the two vacancies in order to increase the symmetry of the model. Test calculations revealed that the choice of the defect position has only a small effect on the stability (less than 0.03 eV). The calculated defect formation energy (with respect to gas-phase Ag atoms) is 3.19 eV/Ag at PW91 level. Due to its high formation energy, this type of defect is rather unlikely under experimental conditions (low temperature). Nevertheless, the generation of point defects during preparation cannot be completely ruled out because part of the energy is regained by putting the atom back on the surface either as single atom or at steps (see below).

Structures close to those described for the perfect surface were chosen as starting points for the adsorption study between defective surfaces. After optimization, it was found that the sulfur atoms of FDT bind to the Ag surface in twofold coordination near the vacancy. Different from the planar surface, where the two adsorption modes are energetically similar, there is a clear preference for adsorption with the Cp axis parallel to the defective surface. For this configuration the reaction energy $\Delta E^{\text{thiolat}}$ is decreased from −0.29 eV (perfect surface) to −1.03 eV (Table I). The structure with the Cp axis perpendicular to Ag(111) is less stable by 0.23 eV.

The Ag(111) surface with *single adatoms* is modeled with a $4\times4\times5$ slab. On both sides of the slab a single silver atom was added at a lattice site above the surface at the same lateral position. This Ag atom is bound to the $4\times4\times5$ slab by −1.95 eV. This reduces the effective Ag formation energy for a single vacancy (previous paragraph) on Ag(111) to 1.24 eV.

The most stable structure of FDT adsorbed between two surfaces with single adatoms is shown in Fig. 1(c): The molecule is rotated so that the sulfur atoms are in close contact with the silver adatom.[32] Although the distance between the Ag slabs has been optimized, too, the sulfur atoms are not exactly on-top of the Ag adatoms. The S–Ag distance (2.43 Å) is the shortest compared with all other configurations tested. However, the interaction energy $\Delta E^{\text{thiolat}} = -0.31$ eV is similar to that on the nondefective surface (Table I). Although energetically not the most favorable configuration, the low coordination of the S atoms for this configuration, which is smaller than in all other configurations tested, leads to significant shifts in the DOS with dramatic consequences in transport, as we will show below.

The $4\times4\times5$ slab was also the basis for the study of *small islands* on the Ag(111) surface. Four silver atoms in a 2×2 arrangement were added on both sides of the slab in a symmetric way. The FDT molecule was placed between the two islands of parallel surfaces in two ways: with the sulfur atoms above the centers of the islands [Fig. 1(d)] and at a side-on position [Fig. 1(e)]. The side-on adsorption turned out to be the most stable geometry of all configurations considered in this study. The interaction energy $\Delta E^{\text{thiolat}} = -1.13$ eV is lower by 0.45 eV than that for adsorption on the island centers (Table I). The side-on adsorption allows the two surfaces to come relatively close to each other. The interlayer distance ΔZ (10.3 Å) is the same as for the Cp-axis-perpendicular adsorption mode between perfect surfaces.

A similar side-on adsorption structure was also studied for the nondissociated ferrocene dithiol. Its stability ($\Delta E^{\text{thiol}} = -0.40$ eV) is similar as for adsorption between two perfect surfaces. The large energetic difference between molecular

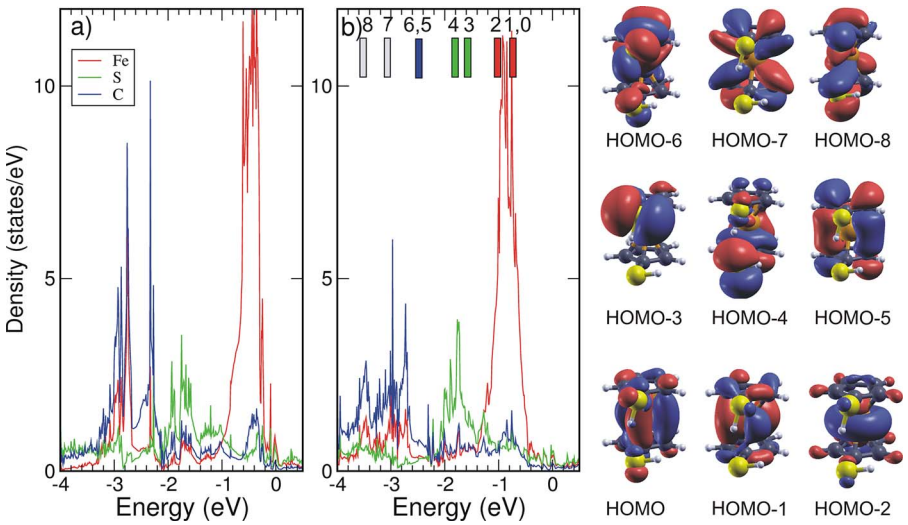

FIG. 2. (Color online) Projected density of states (DOS) of the energetically optimized configurations of FDT adsorbed between two perfect Ag(111) surfaces. The Cp-Fe-Cp axis is close to the parallel orientation with respect to the Ag(111) surface in (a), perpendicular in (b) [see also Figs. 1(a) and 1(b)]. The bars in (b) show the peak positions of the FDT molecule (not the biradical) in the gas phase after a rigid shift to the topmost state. The numbers at the bars correspond to the occupied Kohn-Sham orbitals. Corresponding isosurfaces are shown on the right.

and dissociated forms of FDT at step island and vacancy sites clearly favors dissociation of the S–H bonds on defected Ag surfaces, contrary to the perfect surface.[7] In order to study possible intermediates, the two hydrogen atoms were removed from ferrocene dithiol and adsorbed at adjacent Ag surface atoms. The most stable configuration was more stable than molecularly adsorbed FDT by 0.26 eV. On the defective surface there is a preference for dissociative adsorption. We have not calculated the activation barriers for hydrogen abstraction, but it is assumed that the barriers are moderately large due to the exothermicity.

As an example for a one-dimensional surface defect, we studied FDT adsorption at a *monoatomic step*. A surface supercell was constructed applying the transformation matrix $\binom{3\ -3}{4\ -4}$ to the primitive surface unit cell. The slab consisted of four atomic layers with 24 atoms each in a 6×4 rectangular arrangement. From each of the two outermost layers eight atoms were removed. For a fixed interlayer distance ΔZ the lateral position of the FDT molecule was varied stepwise. This was necessary since the gradient-based optimization routines implemented in VASP do not allow to find the global minimum from an arbitrary starting point. After a systematic search, the minimum structure shown in Fig. 1(f) was found. Similar to the 2×2 island, the FDT prefers to bind to the step edge in a twofold configuration. The reaction energy $\Delta E^{\text{thiolat}}=-0.90$ eV is not as low as for the side-on island adsorption in the previous model with four Ag adatoms. Although this difference may be an indication of a site dependence of the interaction energy, it can also be due to the finite size of the model [see Fig. 1(f)], which prevents the molecule from taking the same optimal side-on position as on the smaller Ag island [Fig. 1(e)]. An indication of the latter effect is the interlayer distance $\Delta Z=11.0$ Å, which is close to the (less favorable) centered adsorption configuration on the 2×2 island.

B. Electronic structure

In this section a direct view on the electronic structure of the adsorbed FDT molecule will first provide direct evidence for molecular adsorption. Since we are interested in the conductive properties of this molecule adsorbed between two Ag electrodes, we focus on the immediate vicinity of the Fermi level of Ag. For electrical conductance, the unoccupied molecular states play no role, since they are more than 2 eV higher in energy.[7] As we will show, changes in coordination and molecular orientation result in subtle modifications of the projected density of states close to the Fermi level, but in substantial differences in the conductive properties. These are quantified by calculations using the nonequilibrium Green's function technique as implemented in the TRANSIESTA code.

As an example, the DOS projected onto different parts of the molecule are shown in Figs. 2(a) and 2(b) for the parallel and perpendicular adsorption geometries on defect-free surfaces, respectively (cf. with Fig. 1). As is clearly seen by this figure, the DOS, starting at the Fermi energy (E_F, zero point) down to −3 eV, is mainly determined by molecular contributions. In this energy range, the DOS projected onto different orbitals of surface and subsurface silver atoms has a comparatively small weight. However, the 3*d* states of Ag(111) contribute significantly to the total DOS starting around −3 eV below E_F (not shown).

These projected DOS turns out to be fully consistent with the assumption of molecular adsorption of the FDT biradical, as demonstrated also in this figure: By shifting the energy scale of the occupied molecular orbitals of the isolated radical rigidly and adjusting it at the highest occupied molecular level (HOMO), we obtained the energy levels indicated by the bars in Fig. 2(b). Also the location of the main electronic density of the isolated radical is consistent with the projections carried out for the adsorbed case. The relative shifts found here are only a few tenth of an eV, indicating a relatively weak contribution of these π-derived molecular orbitals to the bonding of the molecule. This is even valid for the S-derived π orbitals (HOMO-3 and HOMO-4).

As an extreme case, part of these states have even an effective nonbonding character. This is exemplified by the PDOS of the Fe state located at approximately −2.8 eV as shown in Fig. 3 Here the center position of this state is plotted as a function of the binding energy of the molecule. Although the molecular binding varies by a factor of more than 3, the position of this peak stays constant within

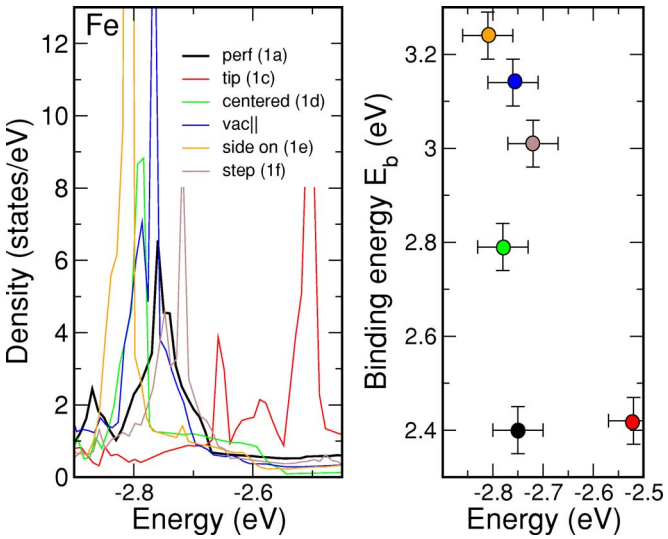

FIG. 3. (Color online) Left: Projected Fe DOS of FDT between two perfect and defective Ag(111) contacts. The numbers in the legend are related to Fig. 1. Right: Peak positions of the Fe peak vs the binding energy for different adsorption geometries. The color code corresponds to the legend, too.

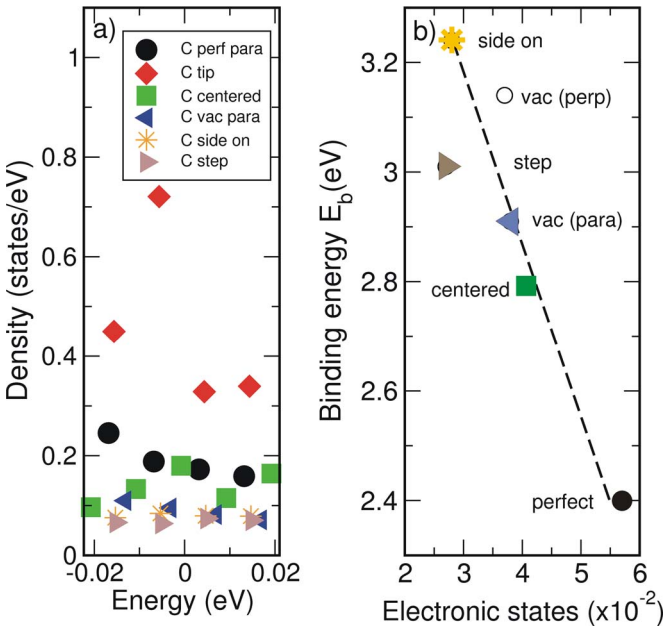

FIG. 4. (Color online) (a) Density of states projected onto the Cp rings close to the Fermi energy for the different adsorption configurations listed in Table I. (b) Correlation between DOS for the different adsorption geometries with a doubly coordinated bond and the binding energy E_b. Here the DOS, obtained with VASP and projected onto the molecule, was integrated over ± 20 meV around E_F. For better visibility the data point of the tip-configuration states is not shown.

± 0.05 eV except for the adsorption on top of a single Ag adatom (tip configuration), where a shift by +0.2 eV was found. Here the bond by the S atom can only be singly coordinated, whereas is all other cases a doubly coordinated bond was found. The small Ag–S adsorption length for the singly coordinated configuration compared to the other configurations (Table I) is a direct consequence. Thus there is a small influence by coordination in this electronic state but not of binding strength.

There is, however, sensitivity to the local coordination in other parts of the PDOS, as obvious from the peak separation to the next peak at higher energy, which depends much more on configuration both in the projections on the Fe and on the Cp rings. This is particularly true close to the Fermi level for all configurations, and can be seen, e.g., also in Fig. 2 for the main part of the Fe 3*d*-derived level that is only a few tenth of an eV below the Fermi energy (red curve). For the geometry with the Cp axis parallel to the surface the onset of the main Fe 3*d* peak is at −0.2 eV, while in the perpendicular adsorption geometry this onset is at −0.5 eV. Since the interaction of the Cp rings with the substrate is higher for latter configuration, the PDOS of the C atoms (blue curve, cf. with HOMO-5 and HOMO-6) around −2.8 eV is broadened and the peaks in the DOS are less pronounced. Broadening seems to be in part also caused by a varying extent of (still small) deformation of the molecule, as seen from a comparison of the different defect configurations. The smallest half widths are observed for the FDT molecule adsorbed at step sites. This configuration seems to allow a configuration closer to its undistorted molecular geometry than the other configurations.

The fact that the projections on both the Fe and the C states change in a similar way demonstrates that the electronic states are extended over the whole ferrocene molecule in this range of energies. This is important in context with the electrical conductance discussed below.

C. Electronic transport

As mentioned, only the occupied electronic states close to the Fermi level are relevant for electrical transport in our case. These states, largely derived from the HOMOs of the isolated radical, are clearly modified by the different bonding configurations investigated here. As expected for orbitals with (slight) bonding character, there is a general downward shift in energy as a function of increasing binding energy, which in most cases, however, is visible only as a change of peak shape of the dominant Fe 3*d*-derived main peak. Thus the DOS at E_F depends both on binding strength and on coordination. Figure 4(a) shows this effect exemplarily for the projection of the DOS onto the Cp rings within a small interval around E_F for all configurations investigated. Projections onto S and Fe atoms have the same tendency. As seen from this figure, there is a significant variation of the electron density in the vicinity of E_F depending on the local atomic configuration. This variation is, as expected, directly correlated with the binding energy E_b of the molecule, as long as the bonding character is similar. As explained above, this is the case for all configurations tested except the adatom (tip) configuration, which will be discussed separately below. In order to demonstrate this correlation, we integrated the PDOS of the C, Fe, and S states over ± 20 meV around E_F and plotted the result in Fig. 4(b) as a function of the binding energy to the Ag surface for all configurations except the adatom configuration. An almost linear dependency is seen, with some deviations for the step and vacancy configurations. In these two configurations, the molecular axis of FDT is almost perpendicular to the surface so that small conformational changes in the molecule compared to the other con-

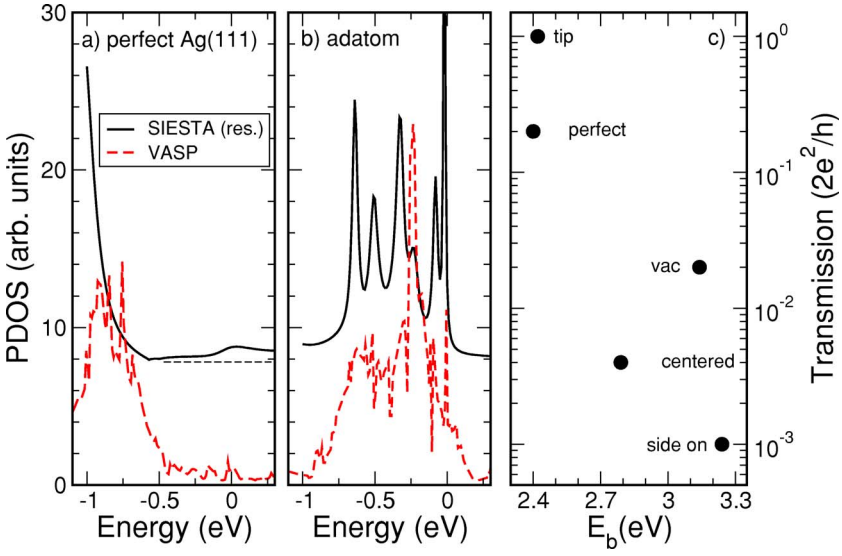

FIG. 5. (Color online) PDOS of the FDT molecule in between perfect (a) and adatom (b) contacts calculated by both SIESTA (solid line) and VASP (dashed line). For better visibility the SIESTA data were rescaled (res.) and shifted. (c) shows the transmission probability as a function of the binding energy. The transmission for the step configuration has not been calculated.

figurations must be expected. These may explain the observed deviations, since already for the adsorption on perfect surfaces the perpendicular configuration turned out to be more sensitive to interactions of the Cp rings with the contact environment. As already mentioned, the S bond in the adatom (tip) configuration is only singly coordinated, and therefore does not fit into this scheme. A high DOS at E_F is seen in this configuration, which is due to the chemical shift induced by the low coordination of the S atom. This causes high electronic transmissions close to unity as we show below.

In order to demonstrate how different chemical environments determine transport properties, the transmission curves for the above mentioned configurations have been computed using TRANSIESTA. The same geometries as those determined as the configurations with minimal energies by VASP were used for these calculations. The quality of the pseudopotential and basis sets for Fe, C, and H during SIESTA/TRANSIESTA calculations have been tested carefully by comparing the electronic structure of the molecule with all-electron calculations based on Gaussian-type TZVP basis set using CRYSTAL code.[28,29] Also, we have compared the binding energy and the potential curves of FDT with respect to the Cp–Cp distance obtained with SIESTA and VASP, and good agreement was found. The pseudopotential and basis sets for Ag and S were taken from other theoretical works.[30,31]

Nevertheless, a direct comparison with full *ab initio* calculations, and especially the prediction of electric transport, which concentrates on a small section of the energy spectrum around the Fermi energy, is still a challenge. Therefore, it was quite satisfying to see that the projected DOS of the FDT molecule obtained by both methods agrees quite well, as shown for the adsorption on the perfect Ag(111) surface (perpendicular orientation) and the adatom contact structure in Figs. 5(a) and 5(b), respectively. These two examples represent the cases of singly and doubly coordinated S–Ag bonds. The increase of the DOS at $E_F-0.7$ eV and below as well as the slight increase in the DOS at E_F for the perfect surface are reproduced by both methods. Even closer agreement is obtained for the adatom structure: Apart from the bandwidth in the energy window shown, also the sharp peak in the DOS at E_F, responsible for high transmission, is reproduced by both TRANSIESTA and VASP. There are of course quantitative differences in the relative intensities and the peaks obtained by VASP are energetically broader. However, the qualitative agreement should allow to see trends in transmittance as a function of coordination and of adsorption strength.

This was done in Fig. 5(c), where we plotted the transmissions at the Fermi energy for the different configurations versus binding energy. Although there is no perfect correlation between transmission and binding energy, there is evidently a qualitative trend of decreasing conductivity with increasing interaction strength. It turns out that the transmittance for adatom configuration corresponds to one conductance quantum, as expected for a singly coordinated bond. In this case no degeneracy is expected so that only one conductance channel is effective at small potential differences between the Ag contacts. This means that this configuration has a fully delocalized state throughout the molecule that extends into the Ag substrate so that an effective coupling is possible. For the doubly coordinated configurations the matching conditions seem to be less perfect, resulting in significantly lower transmission probabilities, which for some configurations are still as high as 0.2. If changes in the density of states at E_F play the dominant role in the transmittance, too, a similar dependence on binding energy as for the DOS should result. Indeed, such a trend is found, as shown in Fig. 5, where transmittance is plotted on a log scale. This may indicate that tunneling processes already play some role, but more detailed quantitative investigations will be necessary before this conclusion can be safely drawn.

Recently we performed transport experiments on this system between ultrasmall Ag contacts, and found a stepwise onset of conductance at a value of 25 μS.[34] This is close to the calculated conductance value for a single FDT molecule in between perfect Ag(111) contacts. However, the contacts used are far from an ideal single crystal,[34] and adsorption is expected to first happen on the energetically most favorable sites, which are the defect sites according to our calculations.

From the anticorrelation between binding energies and conductance found in our calculations, these adsorption configurations are expected to exhibit conductance values which are orders of magnitude lower than those measured. A way around this discrepancy would be the simultaneous adsorption of many molecules, but this is highly improbable. However, this discrepancy can be solved by the following scenario: In the experiment the stepwise increase is typically observed only after longer exposure times of FDT to the contacts. This means that the energetically most favorable sites can be saturated before significant conductance is observed. The adsorption of highly conductive molecules on energetically less favored sites would then be stabilized by a nonzero concentration of FDT molecules already present on the surface. Thus high conductance through single molecules would be only possible by collective stabilization. This interesting scenario still has to be verified by further experiments and calculations.

IV. SUMMARY AND CONCLUSIONS

Using density functional calculations at GGA level, we calculated binding energies of ferrocene dithiol bound to defective Ag(111) surfaces. Zero-dimensional defects (Ag vacancies and adatoms), one-dimensional defects (steps), and two-dimensional defects (small Ag islands) were taken into account. Ferrocene dithiolate preferably binds to two low-coordinated Ag atoms close to vacancies and at islands and steps. The dissociated dithiolate form is much more stabilized than the molecular dithiol form. Thus we conclude that S–H bond dissociation will occur at steps or islands. The strong S–Ag interaction leads to increased splitting of molecular levels, decreases the overlap with the metal levels near the Fermi energy and, finally, reduces significantly the electronic conductivity. From our calculations we conclude that highly conducting single molecules need collective stabilization by a significant amount of FDT molecules, saturating the energetically more favorable, but much less conducting sites on an Ag electrode. Therefore, our future investigations will aim at the effect of lateral interaction between adsorbed ferrocene dithiol molecules on the preferred adsorption site and electronic structure.

ACKNOWLEDGMENTS

We kindly acknowledge Mads Brandbyge and Kongens Lyngby for their help and support with TRANSIESTA. We thank the Höchstleistungsrechenzentrum Nord (HLRN) and the Regionales Rechenzentrum Niedersachsen (RRZN) for providing us with extended CPU time. Part of the structure drawings have been generated with XCrysDen.[33]

[1] R. A. van Santen and M. Neurock, *Molecular Heterogeneous Catalysis* (Wiley-VCH, Weinheim, 2006).
[2] S. A. Ali, M. T. Saeed, and S. V. Rahman, Corros. Sci. **45**, 253 (2003). C. Jeyaprabha, S. Sathiyanarayanan, and G. Venkatachari, Appl. Surf. Sci. **246**, 106 (2005).
[3] U. Landman, W. D. Luedtke, and J. Gao, Langmuir **12**, 4514 (1996).
[4] W. R. Browne and B. L. Feringa, Nat. Nanotechnol. **1**, 25 (2006).
[5] K. H. Müller, Phys. Rev. B **73**, 045403 (2006).
[6] C. Zhang, M.-H. Du, H.-P. Cheng, X.-G. Zhang, A. E. Roitberg, and J. L. Krause, Phys. Rev. Lett. **92**, 158301 (2004).
[7] J. Meyer, T. Bredow, C. Tegenkamp, and H. Pfnür, J. Chem. Phys. **125**, 194705 (2006).
[8] S. A. Getty, C. Engtrakul, L. Wang, R. Liu, S.-H. Ke, H. U. Baranger, W. Yang, M. S. Fuhrer, and L. R. Sita, Phys. Rev. B **71**, 241401 (2005).
[9] G. Esen and M. S. Fuhrer, Appl. Phys. Lett. **87**, 263101 (2005).
[10] J. P. Perdew and Y. Wang, Phys. Rev. B **45**, 13244 (1992).
[11] J. P. Perdew, J. A. Chevary, S. H. Vosko, K. A. Jackson, M. R. Pederson, D. J. Singh, and C. Fiolhais, Phys. Rev. B **46**, 6671 (1992).
[12] G. Kresse and J. Hafner, Phys. Rev. B **47**, 558 (1993).
[13] G. Kresse and J. Hafner, Phys. Rev. B **49**, 14251 (1994).
[14] G. Kresse and J. Furthmüller, Phys. Rev. B **54**, 11169 (1996).
[15] G. Kresse and J. Furthmüller, Comput. Mater. Sci. **6**, 15 (1996).
[16] P. E. Blöchl, Phys. Rev. B **50**, 17953 (1994).
[17] G. Kresse and J. Joubert, Phys. Rev. B **59**, 1758 (1999).
[18] H. J. Monkhorst and J. D. Pack, Phys. Rev. B **13**, 5188 (1976).
[19] M. Methfessel and A. T. Paxton, Phys. Rev. B **40**, 3616 (1989).
[20] O. Dubay, http://cms.mpi.univie.ac.at/odubay/p4vasp_site/.
[21] R. G. W. Wyckoff, *Crystal Structures* (Interscience, New York, 1963).
[22] M. Brandbyge, J.-L. Mozos, P. Ordejón, J. Taylor, and K. Stokbro, Phys. Rev. B **65**, 165401 (2002).
[23] C. Caroli, R. Combescot, D. Lederer, P. Nozieres, and D. Saint-James, J. Phys. C **4**, 2598 (1971); L. V. Keldysh, Sov. Phys. JETP **20**, 1018 (1965); S. Datta, *Electronic Transport in Mesoscopic Systems* (Cambridge University Press, Cambridge, 1995).
[24] J. M. Soler, E. Artacho, J. D. Gale, A. Garcia, J. Junquera, P. Ordejon, and D. Sanchez-Portal, J. Phys.: Condens. Matter **14** 2745 (2002).
[25] J. P. Perdew, K. Burke, and M. Ernzerhof, Phys. Rev. Lett. **77**, 3865 (1996).
[26] For simplicity the unsubstituted ferrocene structure is assumed to classify the adsorption modes.
[27] F. Ortmann, F. Bechstedt, and W. G. Schmidt, Phys. Rev. B **73**, 205101 (2006).
[28] TURBOMOLE basis set library for iron. ftp://ftp.chemie.uni-karlsruhe.de/pub/basen/fe.
[29] V. R. Saunders, R. Dovesi, C. Roetti, R. Orlando, C. M. Zicovich-Wilson, N. M. Harrison, K. Doll, B. Civalleri, I. J. Bush, Ph. D'Arco, and M. Llunell, *CRYSTAL2003 User's Manual* (University of Turin, Turin, 2003).
[30] J. Izquierdo, A. Vega, L. C. Balbás, D. Sánchez-Portal, J. Junquera, E. Artacho, J. M. Soler, and P. Ordejón, Phys. Rev. B **61**, 13639 (2000).
[31] M. Paulsson, T. Frederiksen, and M. Brandbyge, Nano Lett. **6**, 258 (2006).
[32] In principle such a configuration is also possible for the nondefective surface, and has been tested for the nondissociated FDT molecule. The reaction energy ΔE^{thiol} for the rotated geometry (−0.32 eV) is between the values for parallel and perpendicular orientations (−0.36 and −0.23 eV, see Table I).
[33] A. Kokalj, J. Mol. Graphics Modell. **17**, 176 (1999).
[34] G. Gardionowski, J. Schmeidel, H. Pfnür, T. Block, and C. Tegenkamp, Appl. Phys. Lett. **89**, 063120 (2006).